ECCM 11
11th European Conference on Composite Materials
May 31 – June 3 2004, Rhodes (Greece)

EXPERIMENTAL AND NUMERICAL DETERMINATION OF THE MECHANICAL PROPERTIES OF MULTI-AXIAL MULTI-PLY COMPOSITES

*V. Carvelli, **T. Truong Chi, *M. S. Larosa, **S. V. Lomov,
*C. Poggi, ***D. Ranz Angulo, **I. Verpoest

*Department of Structural Engineering, Technical University (Politecnico)of Milan,
Piazza Leonardo Da Vinci 32, 20133 Milan (Italy)

**Department MTM, Katholieke Universiteit Leuven,
Kasteelpark Arenberg 44, B-3001 Leuven (Belgium)

***Facultad de Ciencias, University of Zaragoza,
Pedro Cerbuna 12, 50009 Zaragoza (Spain)

ABSTRACT

The paper presents the experimental and numerical investigation methods adopted to evaluate and predict the mechanical response of multi-axial multi-ply carbon stitched laminates. An accurate experimental mechanical investigation was carried out in accordance to international standards at MTM Laboratory in Leuven. The numerical approach, developed and implemented by the Milan group, consists of two-scale homogenisation, based on the assumption of regular distribution of the fibres in the layer and of the stitching in the laminate. The channels produced by the stitching are included in the finite element model of the material Representative Volume (RV). The complete tensile behaviour of the composites was simulated and compared to the experimental results.

Keywords: multi-axial multi-ply composites, stitching, mechanical properties, experimental tests, numerical predictions.

INTRODUCTION

Multi-axial multi-ply composites are obtained as combination of uni-directional plies with transversal consolidation by stitching. This technique allows to better exploit the material properties since a full use of the stiffness and strength of the fibres is possible. Furthermore the use of the Resin Transfer Moulding technique is made possible.
The research activity deals with an experimental and numerical investigation to evaluate and predict the mechanical response of carbon stitched laminates.
Two different laminates were considered: a quadriaxial laminate with stacking sequence $(45°/90°/-45°/0°/0°/-45°/90°/45°)_S$, and a biaxial laminate with layout (45°/-45°/45°/-45°/-45°/45°/-45°/45°).
For both materials an experimental investigation was carried out in accordance to international standards. A complete mechanical experimental characterization was performed at MTM Laboratory in Leuven. Some results are discussed in the next section (see also ref. [1]).

The numerical approach (implemented by the Milan group) is based on two-scale homogenisation technique. Assuming the hypothesis of regular distribution of the fibres in the layer and of the stitching in the laminate, the homogenization theory for heterogeneous periodic materials is applied. The periodicity is enforced by particular boundary conditions in both steps. In the first homogenisation procedure the lamina is considered as a periodic unidirectional composites and the mechanical properties are obtained studying an hexagonal Representative Volume fairly small cell comprising a single fibre and the surrounding matrix (the RV dimensions are of the order of microns). The results are obtained by the numerical approach proposed in [2]. The second homogenisation step concerns the laminate, in which each lamina is considered as a homogenized material with the mechanical properties obtained in the first homogenisation step [3]. The numerical analysis of the RV allows to predict both the elastic properties and the failure behaviour. The procedure to simulate the progressive damage of the material is similar to the model proposed by Zako et al. in [4, 5].
The numerical model includes the real geometry of the plies and of the stitching measured at MTM Laboratory in Leuven [6]. An important feature of the geometry is imperfections ("cracks" and "channels") introduced in the plies by the stitching.
The elastic properties were predicted for both the laminates. The complete tensile behaviour was simulated both considering a perfect laminate (no stitching) and a laminate in which the channels produced by the stitching were modelled. The geometry of the channels in each layer was deduced by microscopic average measurements [6] and in the finite element representation they were filled with the matrix material.

EXPERIMENTAL INVESTIGATION

Geometric measurements

FE model of the plies was constructed according to the geometrical data in Table 1 (see Figure 1 for geometric parameters of stitching and channels), measured elsewhere [7].

	Quadriaxial [mm]	**Biaxial** [mm]
Spacing of the stitching		
along the needles, A	5.09	4.94
machine direction, B	2.58	1.71
Width of channels/cracks in the preform		
face of the preform	0.66	0.27
middle plies	0.18	n/a
back of the preform	0.48	0.43
Length of cracks in the preform		
face of the preform	n/a	5.05
middle plies	2.1	n/a
back of the preform	5.8	7.20
Gap between layers	0.05	0.05

Table 1: Geometrical parameters of the reinforcement.

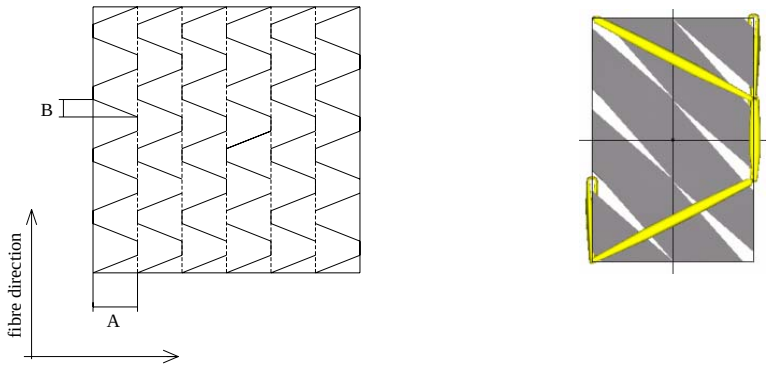

(a) (b)

Figure 1: (a) Stitching pattern of the quadriaxial laminate; (b) channels/cracks geometry for 45° ply.

Tensile tests

Tensile tests were performed on quadriaxial and biaxial laminates in machine direction (MD), bias direction (BD) and cross direction (CD) to determine the elastic modulus (E), Poisson ratio (ν), stress (σ_f) and strain (ε_f) at failure. The stress-strain curves were also obtained. More details on experimental investigation can be found in [1].
The standard ISO 527-4 "Test conditions for isotropic and anisotropic fibre reinforced plastic composites" was followed to prepare the specimens and perform the tensile test. An Instron 4505 with hydraulic clamping was used as testing equipment. The crosshead speed was set at 1mm/min. A load cell of 100kN was used to measure the force. Two extensometers with a gauge length of 50mm and 12.5mm respectively were placed on the specimen to register the displacement in both length and width directions during the test. The specimen dimensions were 250mm by 12.5mm. The tensile properties of the quadriaxial and biaxial laminates in different directions are shown and compared in Table 2, in which the fibre volume fraction V_f of the specimens is listed. As expected, quadriaxial laminates show a quasi-isotropic behaviour, while the biaxial laminates clearly present an anisotropic behaviour.

Material	**Test direction**	**E** [GPa]	**σ_f** [MPa]	**ε_f** [%]	**ν**	**V_f** [%]
Quadriaxial	Machine	32.8±0.6	530±26	1.76±0.10	0.30±0.02	42.1±0.8
	Bias	32.5±0.9	496±26	1.81±0.05	0.33±0.02	40.3±2.5
	Cross	34.1±1.3	500±23	1.61±0.09	0.37±0.05	44.5±1.2
Biaxial	Machine	9.9±0.4	177.4±3.9	8.7±0.3	0.83±0.04	39.4±1.8
	Bias	44.8±4.2	689.0±47	1.6±0.1	0.05±0.01	39.4±1.8
	Cross	9.5±0.4	159.7±1.7	9.4±0.9	0.82±0.04	36.9±1.1

Table 2: Tensile properties of quadriaxial and biaxial fabrics epoxy reinforced composites in different directions.

For damage investigation in the laminates under consideration, the acoustic emission (AE), namely the Wave Explorer system, was integrated in tensile tests. Two acoustic emission sensors were attached 30mm away from the longitudinal extensometer to collect acoustic signals generated during the test. They also make it possible to determine the velocity of the sound in the material, hence to localise the source. X-Ray equipment Philips HOMX together

with AEA Tomohawk software were used to detect damage in the specimens after tensile loading. The AE events versus strain and stress versus strain obtained from tensile test on quadriaxial and biaxial laminates are depicted in Figure 2 and Figure 3 respectively. The damage for quadriaxial laminate starts at strain between 0.2 to 0.4%; the biaxial laminate shows damage beginning at strain between 0.1 to 0.3% for the BD traction and at strain 1.3% for the MD test.

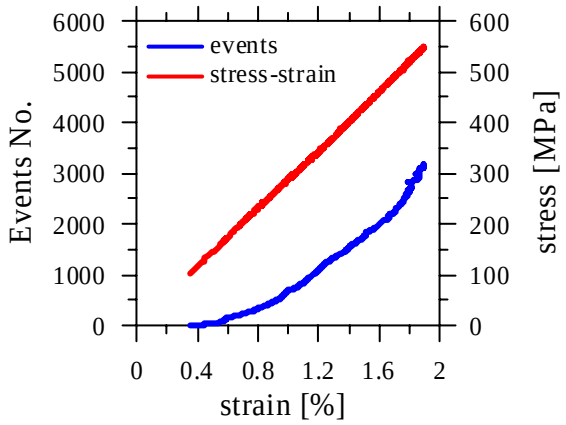

Figure 2: AE events versus strain and stress versus stress obtained from MD tensile test on quadriaxial laminates.

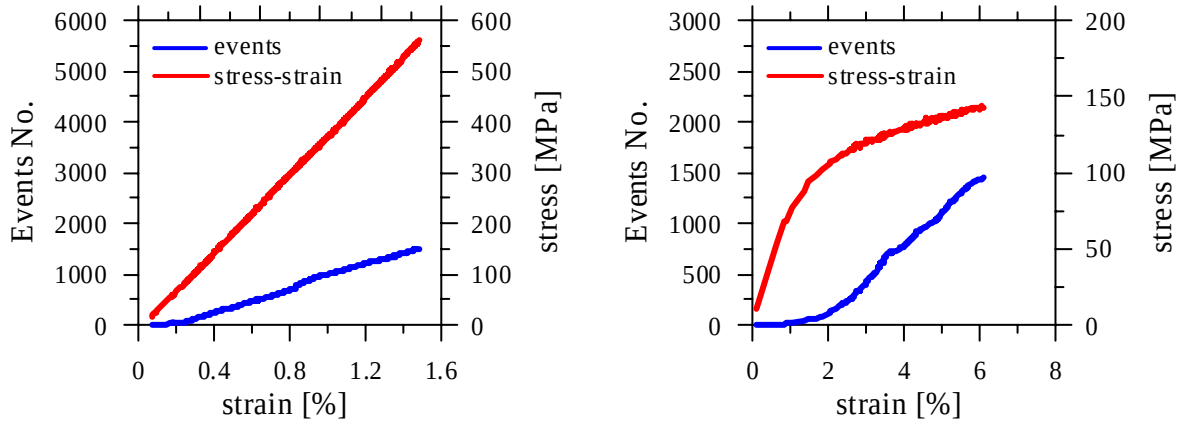

Figure 3: AE events versus strain and stress versus stress obtained from tensile test on biaxial laminates for: (a) BD traction; (b) MD traction.

Shear tests

ASTM D5379/D5379M–93 “Standard test method for shear properties of composite materials by the V-notched beam method” was used to prepare the specimens and perform the test to measure in plane shear properties of the materials: shear modulus (G), shear strength (τ_u). The Instron 1196 and V-notched beam test fixture were used in the tests. Strain gauges with an active gauge length of 3mm were used to measure shear strain. The cross-head speed was set at 1mm/min. A load cell of 20kN was used. According to the standard, the quadriaxial laminate was tested in machine direction while the biaxial laminate was tested in bias direction. The specimen dimensions were 76mm by 19mm and 3.4mm thick. Three mm thick end tabs were used to strengthen and stabilise the specimens. They also help to prevent the specimens from compression failure.

Table 3 shows the in plane shear properties of quadriaxial and biaxial laminates. The fibre volume fraction V_f of the specimens is also listed The quadriaxial laminate has the higher shear strength and modulus. It is evident because the material was reinforced by +45° and –45° layers, which significantly enhance the shear properties.

Material	**G** [GPa]	**τ_u** [MPa]	**V_f** [%]
Quadraxial (MD)	11.3±0.8	222.0±13.9	42.1±0.8
Biaxial (BD)	3.3±0.3	61.5±4.8	39.4±1.8

Table 3: the in plane shear properties of quadriaxial and biaxial laminates.

NUMERICAL HOMOGENIZATION PROCEDURE

Problem Formulation

A three-dimensional numerical approach was implemented by the Milan group to evaluate the mechanical features of multi-axial multi-ply stitched composites. The main hypotheses are: (i) regular distribution of the fibres in the plies; (ii) regular arrangement of the stitching path in the composites. These allows to work in the framework of the homogenization theory for periodic media [8]. The numerical analyses consists in a two-scale homogenisation: the first at the ply level and the second at the laminate level.

A perfect link between fibres and matrix and between the layers is assumed. The last hypothesis is a limitation and could be removed introducing interfaces to transmit forces both between the fibres and the matrix in the ply and between plies.

The macroscopic constitutive law describes the relation between macroscopic stresses and strains vectors ($\underline{\underline{\Sigma}}$, $\underline{\underline{E}}$)**,** defined as volumetric averages of the relevant microscopic variables ($\underline{\underline{\sigma}}(\underline{x})$, $\underline{\underline{\varepsilon}}(\underline{x})$) that are functions of the position vector $\underline{x}$ in the representative volume (RV). In both homogenization scales the macroscopic constitutive law is determined in incremental form solving the problem:

$$\operatorname{div}\dot{\underline{\underline{\sigma}}} = \underline{\underline{0}} \quad \text{in } V; \qquad \dot{\underline{\underline{\sigma}}} = F(\dot{\underline{\underline{\varepsilon}}}(\dot{\underline{u}})) \quad \text{in } V \tag{1a,b}$$

$$\tilde{\dot{\underline{u}}} = \dot{\underline{u}} - \dot{\underline{\underline{E}}} \cdot \underline{x} \quad V - \text{periodic}; \qquad \dot{\underline{t}} = \dot{\underline{\underline{\sigma}}} \cdot \underline{n} \quad \text{anti - periodic on } \partial V \tag{1c,d}$$

$$\dot{\underline{\underline{\Sigma}}} = \frac{1}{V}\int_V \dot{\underline{\underline{\sigma}}} dV; \qquad \dot{\underline{\underline{E}}} = \frac{1}{V}\int_V \dot{\underline{\underline{\varepsilon}}} dV \tag{1e,f}$$

where ∂V and V indicate the boundary and the volume of the RV; $\underline{n}$ is the outward unit-normal to ∂V. Eqn. (1a) is the microscopic equilibrium equation; eqn. (1b) represents the microscopic incremental constitutive law while eqn. (1c) and eqn. (1d) are the periodic kinematics and static boundary conditions respectively. The definition of the macroscopic quantities ($\underline{\underline{\Sigma}}$, $\underline{\underline{E}}$) is expressed by eqns. (1e,f).

Boundary conditions

In order to fulfil the assumed two-scale periodicity of the heterogeneous material, in terms of kinematic quantities, the following general relation of the displacement field (1c) holds:

$$\underline{u}(\underline{x}) = \underline{u}^0 + \underline{\underline{\Omega}} \cdot \underline{x} + \underline{\underline{E}} \cdot \underline{x} + \underline{\tilde{u}}(\underline{x}) \tag{2}$$

where $\underline{u}^0$ represents a rigid displacement of the RV and $\underline{\underline{\Omega}}$ is the anti-symmetric tensor related to the small rigid rotation of the RV. The pure strain modes of the RV are described by the last two terms in (2): a constant term (the macroscopic strain $\underline{\underline{E}}$) and a *V*-periodic term, with zero average value, associated with the *V*-periodic part $\underline{\tilde{u}}$ of the microscopic displacement field.

The main task to implement problem (1) in a displacement formulation FE code is the assignment of the boundary conditions to ensure that the displacement field complies with eqn. (2). Details on the boundary conditions applied to the hexagonal RV used in the first scale modelling of the present approach are described in ref. [2]. On the other hand, the periodic displacement boundary conditions applied to the RV implemented in the second scale level are defined in [3]. In ref. [2, 3] are detailed the kinematic boundary conditions to simulate any prescribed macroscopic strain through only some free nodal displacement components. In the numerical simulations macroscopic strain components are prescribed and the macroscopic stress tensor is evaluated by the volumetric averages (1e,f) of the microscopic counterparts in the Gauss integration points.

Failure prediction

The progressive damage of the stitched laminate composite is predicted, in the second scale analysis, assuming the Tsai-Hill failure criteria for the anisotropic homogenized layers [9]. The strength parameters of the homogenized layers for Tsai-Hill domain are evaluated by the first scale model assuming a transversally isotropic carbon fibre and an isotropic matrix.

A simple degradation procedure is applied to evaluate the damage in the layers up to complete failure. When the stress state in a element satisfies the assumed failure criterion, some stiffness matrix elements are dropped down according to the failure mechanism involved. The considered failure mechanics were presented by Zako et al. [4, 5]. Four possible damage modes are taken into account (see Table 4). Mode 1 represents the fibre breakage (being 1 the fibre direction); Modes 2 and 3 are due to transverse failure by normal stress and Modes 13, 23, 12 provide shear cracking.

Damage mode	Mode 1 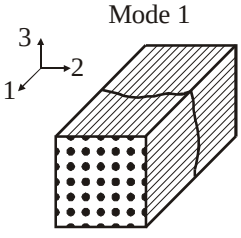	Mode 2 or 12 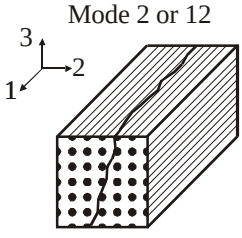	Mode 3 or 13 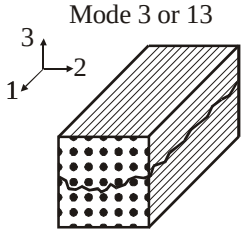	Mode 23 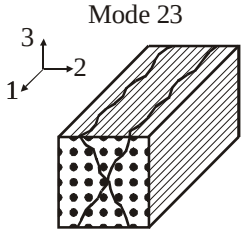
Maximum stress-strength ratio	$\frac{\sigma_1^2}{F_1^t F_1^c}$	$\frac{\sigma_2^2}{F_2^t F_2^c}$ or $\left(\frac{\tau_{12}}{F_{12}^s}\right)^2$	$\frac{\sigma_3^2}{F_3^t F_3^c}$ or $\left(\frac{\tau_{13}}{F_{13}^s}\right)^2$	$\left(\frac{\tau_{23}}{F_{23}^s}\right)^2$

Table 4: damage modes for plies and maximum stress-strength ratio correlation.

The activation of a failure mode is assumed to depend on the maximum stress-strength ratio. The correlation between damage modes and stress-strength ratios is detailed in Table 4 where F^t, F^c, F^s are the tensile, compressive and shear strength parameters of the yarns (in the numerical analyses is assumed $F^t = F^c$).

The components of the stiffness matrix to be reduced depend on the active damage mode. In Table 5 the reduction schemes associated to each damage mode are described. The damage parameter d is assumed equal to 0.001.

Damage mode	Mode 1	Mode 2 or 12
reduced stiffness matrix	$\begin{bmatrix} dQ_{11} & dQ_{12} & dQ_{13} & 0 & 0 & 0 \\ & Q_{22} & Q_{23} & 0 & 0 & 0 \\ & & Q_{33} & 0 & 0 & 0 \\ & sym. & & dQ_{44} & 0 & 0 \\ & & & & dQ_{55} & 0 \\ & & & & & Q_{66} \end{bmatrix}$	$\begin{bmatrix} Q_{11} & dQ_{12} & Q_{13} & 0 & 0 & 0 \\ & dQ_{22} & dQ_{23} & 0 & 0 & 0 \\ & & Q_{33} & 0 & 0 & 0 \\ & sym. & & dQ_{44} & 0 & 0 \\ & & & & Q_{55} & 0 \\ & & & & & dQ_{66} \end{bmatrix}$

Damage mode	Mode 3 or 13	Mode 23
reduced stiffness matrix	$\begin{bmatrix} Q_{11} & Q_{12} & dQ_{13} & 0 & 0 & 0 \\ & Q_{22} & dQ_{23} & 0 & 0 & 0 \\ & & dQ_{33} & 0 & 0 & 0 \\ & sym. & & Q_{44} & 0 & 0 \\ & & & & dQ_{55} & 0 \\ & & & & & dQ_{66} \end{bmatrix}$	$\begin{bmatrix} Q_{11} & dQ_{12} & dQ_{13} & 0 & 0 & 0 \\ & dQ_{22} & dQ_{23} & 0 & 0 & 0 \\ & & dQ_{33} & 0 & 0 & 0 \\ & sym. & & dQ_{44} & 0 & 0 \\ & & & & dQ_{55} & 0 \\ & & & & & dQ_{66} \end{bmatrix}$

Table 5: reduced stiffness matrix components depending on the active damage mode.

EXPERIMENTAL AND NUMERICAL COMPARISONS

The numerical procedure is applied to predict the elastic properties of the biaxial and quadriaxial laminates without stitching and the complete behaviour until failure of the quadriaxial laminate including the channels produced by stitching. The numerical results are compared to the experimental observations.

The aim of the first-scale homogenisation (at the ply level) is to obtain the elastic and ultimate properties of the plies. The numerical approach proposed in [2] was used assuming von Mises and Hill failure behaviour for the matrix and carbon fibre respectively. The mechanical properties of the unidirectional plies was computed assuming the fibre volume fraction of the laminate listed in Table 2 and introducing the properties of carbon fibre and resin matrix reported in and Table 6a and Table 6b.

The second-scale homogenisation was performed at the multi-ply composite level taking into consideration the homogenized layers from the first-scale analysis. A commercial finite element code was used [10]. The RV of the multi-ply composite without stitching influence is discretized by 4913 nodes and 4096 3D-8 nodes elements, while the RV of the multi-ply composite with stitching channels has 71120 tetrahedral elements and 13447 nodes (see Figure 4).

$E_{22}=E_{11}$ [GPa]	E_{33} [GPa]	G_{12} [GPa]	$G_{13}=G_{23}$ [GPa]	ν_{12}	$\nu_{13}=\nu_{23}$	$\sigma_{f22}=\sigma_{f11}$ [MPa]	σ_{f33} [MPa]	$\varepsilon_{f22}=\varepsilon_{f11}$ [%]	ε_{f33} [%]
72	238	28	86	0.30	0.27	1777	3950	0.405	1.5

(a)

E [GPa]	ν	σ_f [MPa]	ε_f [%]
2.73	0.4	70.13	4.09

(b)

Table 6: mechanical properties of: (a) transverse isotropic carbon fibre (been 3 the longitudinal fibre direction); (b) isotropic matrix

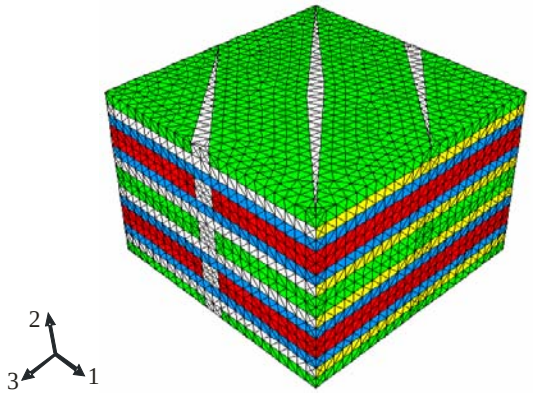

Figure 4: Finite Element model of the quadriaxial laminate Representative Volume.

The results of elastic analyses on quadriaxial and biaxial laminates are listed in Table 7. The stitching channels were not taken into consideration (perfect laminate). The comparison with experimental results shows an overestimation of the numerical properties for the quadriaxial laminate and an underestimation for the biaxial laminate. In Table 7 and in the following, MD corresponds to axis 3 and CD to axis 1 (see Figure 4).

	Quadriaxial			**Biaxial**		
	FE-RV	**Experimental**	**V_f**	**FE-RV**	**Experimental**	**V_f**
E_1 [GPa]	39.82	32.8	0.445	7.38	9.48	0.3696
E_3 [GPa]	37.52	31.2	0.4212	7.81	9.92	0.3943
ν_{13}	0.372	0.30	0.4212	0.839	0.83	0.3943
G_{13} [GPa]	14.85	10.25	0.445			

Table 7: FE and experimental elastic properties of the (a) quadriaxial and (b) biaxial laminates without stitching channels.

The complete mechanical behaviour until failure of the quadriaxial laminate is predicted by the proposed numerical approach. The analyses are performed with the perfect laminate and the stitched material in which the geometry of the channels fulfil the measurements. In the

RV, the transversal stitching channels (along 2 axis, see Figure 4) are considered, filled by the matrix material, while the channels in the plane 1-3 and the stitching fibres are not taken into consideration.
The numerical simulations provide the results depicted in Figure 5 for a traction along the directions: MD (Figure 5a) and CD (Figure 5b). The numerical macroscopic stress-strain relations lies above (perfect laminate) and below (with stitching channels) the experimental tests respectively. In fact, the numerical results identify a narrow zone in which the experimental curves are contained. Taking into consideration some of stitching channels the numerical model predicts a constitutive behaviour of the laminate close to the experimental one, in term of elastic modulus and failure stress.
The numerical stress-strain curve for MD traction of the RV with channel starts to change slope in a strain range very similar to the AE estimation (0.2÷0.3) (see Figure 2 and Figure 5a). This means that, in some integration points the stress state reach the boundary of the failure domain and the damage starts to develop in the material according to the damage modes in Table 4.

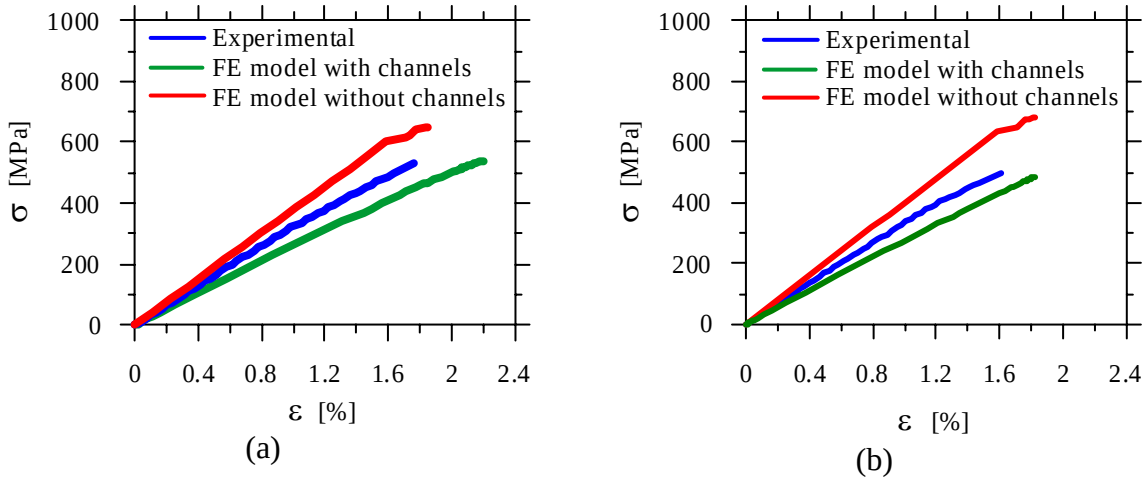

Figure 5: Comparisons of the macroscopic stress-strain behaviour by the present approach and experiments. Tensile test in direction: (a) MD; (b) CD.

CONCLUSIONS

An experimental investigation and a numerical procedure to study the mechanical properties of multi-axial multi-ply carbon stitched laminates has been presented. MTM of KU Lueven and Milan research teams developed the experimental and the numerical investigation respectively.
The material properties of the plies were numerically computed in the first homogenisation scale. The real geometry of the plies, including the stitching shapes, was used in the second homogenisation model. The results of the two-scale homogenisation method were compared to the experimental investigation. In particular, tensile tests in different directions were simulated and the comparisons between the elastic properties and the failure behaviour were satisfactory. The experimental tensile behaviour lies in the narrow zone defined by the numerical simulations referred to a perfect laminate (without stitching) and a laminate with channels produced by the stitching process.

REFERENCES

1. Truong Chi, T., Vettori, M., Lomov, S. V., Verpoest, I., “New results on mechanical properties and initial damage of multi-axial multi-ply carbon fabrics reinforced epoxy”, Proc. ECCM-11, May 31 – June 3 2004, Rhodes (Greece).
2. Carvelli, V., Taliercio, A., “A Micromechanical model for the analisys of unidirectional elastoplastic composites subjected to 3D stresses”, Mechanics Research Communications, 26/5 (1999), 547-553.
3. Carvelli, V., Poggi, C., “A homogenization procedure for the numerical analysis of woven fabric composites”, Composite Part A, 32/10 (2001), 1425-1432.
4. Zako, M., Tanako, N., Uetsuji, Y., “Predicting of strength for fibrous composites based on damage mechanics”, Proc. TEXCOMP-3, 9-11 December 1996, Aechen (Germany).
5. Zako, M., Uetsuji, Y., Kurashiki, T., “Finite element analysis of damaged woven fabric composite materials”, Composite Science and Technology, 63 (2003), 507-516.
6. Lomov, S.V., Belov, E.B., Bischoff, T., Ghosh, S.B., Thanh, T.C., Verpoest, I., “Carbon composites based on multi-axial multi-ply stitched performs - Part 1: Geometry of the perform”, Composites A, 33/9 (2002), 1171-1183.
7. Lomov, S.V., Verpoest, I., Peeters, T., Roose, D., Zako, M., “Nesting in textile laminates: Geometrical modelling of the laminate”, Composites Science and Technilogy, 63/7 (2003), 993-1007.
8. Suquet, P., “Elements of homogenization for inelastic solid mechanics”, In E. Sanchez-Palencia and A. Zaoui eds. ‘Homogenization techniques for composite media’, Lecture Notes in Physics 272, Springer, Wien, 193-278, (1985).
9. Herakovich, C. T., “Mechanics of fibrous composites”, John Wiley & Sons, (1998).
10. ABAQUS release 6.4, user’s manual, (2003).